Supplemental Materials

Antigen-loaded monocyte administration induces potent therapeutic anti-tumor T cell responses

Min-Nung Huang[1,2], Lowell T. Nicholson[3], Kristen A. Batich[3,4,5], Adam M. Swartz[4,5], David Kopin[3], Sebastian Wellford[1], Vijay K. Prabhakar[3], Karolina Woroniecka[3,4,5], Smita K. Nair[4,5,6,7], Peter E. Fecci[4,5,6], John H. Sampson[4,5,6], Michael D. Gunn[1,2*]

[1]Department of Immunology, [2]Division of Cardiology, Department of Medicine, [3]School of Medicine, [4]Department of Pathology, [5]Preston Robert Tisch Brain Tumor Center, [6]Department of Neurosurgery, [7]Department of Surgery, Duke University Medical Center, Durham, North Carolina 27710, USA
*Corresponding author

Supplemental Methods

Antibodies and the tetramers. The antibodies used for cell purification include anti-CD3ε (eBio500A2), CD4 (GK1.5), CD8α (53-6.7), CD19 (MB19-1), B220 (RA3-6B2), CD49b (DX5), TER-119 (all from eBioscience); CD11b (M1/70), CD11c (HL3), Ly-6G (1A8), I-A^b (AF6-120.1), Sca-1 (E13-161.7), c-Kit (2B8; all from BD Pharmingen); and CCR3 (83101; R&D). Anti-CCR3 is FITC-conjugated and anti-Ly-6G is FITC-conjugated or biotinylated while all the others are biotinylated. For cell phenotyping and FACS cell sorting, the antibodies conjugated to FITC, PE, PE-Cy5.5, PE-Cy7, APC, eFluor 660, APC-Cy7, BV421, V450, Pacific Blue, AF700, eFluor 605NC, BV605, BV650, eFluor 650NC, BV711 or BV786 and specific to the following mouse antigens were used: CD3ε (145-2C11), CD4 (GK1.5 or RM4-5), CD14 (Sa14-2), CD25 (PC61), CD44 (IM7), CD45 (30F-11), CD45.2 (104), CD115 (AFS98), B220 (RA3-6B2), F4/80 (BM8), IFNγ (XMG1.2; all from BioLegend); CD8α (53-6.7), CD11c (N418), CD19 (eBio1D3), CD49b (DX5), CD86 (GL1), F4/80 (BM8), NK1.1 (PK136), I-A/I-E (M5/114.15.2), Eomes (Dan11mag), Granzyme B (NGZB), T-bet (eBio4B10; all from eBioscience); CD11b (M1/70), CD40 (3/23), CD45.1 (A20), CD62L (MEL-14), Ly-6C (AL-21), Ly-6G (1A8), Vα2 (B20.1; all from BD Pharmingen). Isotype control antibodies were from the corresponding sources. Anti-mouse CD16/32 (93; functional grade, eBioscience) was used for FcγR blocking. PE-Cy7-conjugated anti-human CD3 (OKT3) was from BioLegend. PE-conjugated SIINFEKL- and $TRP_{180\text{-}188}$-H-$2K^b$ tetramers were from MBL International. AF488-conjuated annexin V and propidium iodide (PI) for apoptosis staining were from Invitrogen.

Flow cytometry and cell sorting. Cells were stained with antibodies for 30 min at 4°C in PBS containing 3% FBS, 5 μg/ml of anti-CD16/32, 5% normal rat serum, 5% normal mouse serum and 10 mM EDTA. Intracellular staining was done after surface staining with BD Cytofix/Cytoperm™ kit (BD Biosciences) according to the manufacturer's instructions. Apoptosis staining was performed with AF 488-conjugated annexin V and PI (Invitrogen) per manufacturer's instructions. Tetramer staining was performed for 30 min at room temperature. Dead cells were identified with LIVE/DEAD Fixable Aqua Dead Cell Stains (Molecular Probes) or 7AAD (eBioscience) and excluded from analysis. Flow cytometric data was acquired using a LSRII flow cytometer (BD Biosciences) and analyzed using FlowJo software (Tree Star). For splenic cDC sorting, spleens were minced and digested in HBSS containing 5% FBS, 10mM

HEPES with collagenase A (1 mg/ml; Roche) and DNase I (0.4 mg/ml; Roche) for 30 min at 37°C, passed through a 70 μm Nylon cell strainer (Falcon), and resuspended in HBSS containing 5% FBS, 10 mM HEPES and 10 mM EDTA. Red blood cells (RBCs) were lysed with ACK lysis buffer. To obtain DC-enriched splenocytes, cells were incubated with biotinylated Ly-6G/Gr-1 (RB6-8C5; eBioscience), CD19, B220 and CD3 (all at 1.25 μg/ml) for 30 min at 4°C, followed by a 15-minute incubation with streptavidin-conjugated MACS magnetic MicroBeads (Miltenyi) at 4°C. The cells were negative selected via MACS LD columns (Miltenyi). The effluent cells were further surface stained with anti-CD11c, CD45, CD8, I-A/I-E and 7AAD. High purity (>95%) splenic cDC were sorted from $CD11c^+$I-A/I-$E^+CD45^+7AAD^-$ cells on a FACS Aria II cell sorter (BD Biosciences). The resulting splenic cDC were composed of $CD8^+CD11b^-$ cDC (~25%) and $CD8^-CD11b^+$ cDC (~75%), both of which were also FACS-sorted as needed based on CD8 expression. For naïve T cell sorting, spleens from OT-I or OT-II mice were minced, the cell suspensions RBC-lysed, passed through a 70 μm Nylon cell strainer (Falcon), and stained with anti-Vα2, CD62L, CD44, CD8 (for OT-I), CD4 (for OT-II), CD25 and 7AAD (eBioscience). High purity (>95%) naïve OT-I or OT-II cells were sorted from $Vα2^+CD62L^{hi}CD44^{lo}CD25^-7AAD^-$ $CD4^+$(OT-II) or $CD8^+$(OT-I) cells by a MoFlo XDP sorter (Beckman Coulter).

Restimulation of total splenocytes with PMA and ionomycin. Total splenocytes were isolated from mice vaccinated 7 days earlier with IV OVA-loaded monocytes (4×10^6 per mouse), SQ OVA/CFA (1:1 emulsion; 200 μg OVA/200 μl per mouse; Sigma) or SQ PBS/CFA (1:1 emulsion; 200 μl per mouse; Sigma) and were cultured at 5×10^6/ml for 4 hours in cRPMI-10 medium containing 50 μM 2-mercaptoethanol (2-ME), PMA (50 ng/ml; Abcam), ionomycin (500 ng/ml; Sigma), brefeldin A (BD Biosciences) and monensin (eBioscience) with 5% CO_2 at 37°C. Cells were then washed and stained with SIINFEKL-H-$2K^b$ tetramer, followed by Aqua Dead cell staining, surface staining and intracellular staining with anti-Eomes, T-bet, Granzyme B and IFNγ. Live $tetramer^+CD8^+$ T cells were gated for further analysis of effector functions.

In vivo CTL assay. Measurement of CTL activity in vivo was performed as previously described (1) with some modifications. In brief, target cells were prepared from RBC-depleted naïve syngeneic splenocytes with or without SIINFEKL peptide pulsing (1 μg/ml for 45 min at 37°C). SIINFEKL-pulsed and -unpulsed splenocytes were labeled with CFSE at high (5 μM; $CFSE^{high}$) and low concentrations (0.5 μM; $CFSE^{low}$) respectively. $CFSE^{high}$ and $CFSE^{low}$ cells were mixed well at a 1:1 ratio and were thoroughly washed with PBS before use. A total of $10x10^6$ cells ($5x10^6$ from each population) in 50 μl PBS were IV injected in each recipient mouse immunized 7 days earlier with IV OVA-loaded monocytes ($4x10^6$ per mouse), SQ OVA/CFA (200 μg OVA /200 μl) or SQ PBS/CFA (200 μl). Spleens were harvested 6 hours later from recipient mice and single-cell suspensions were prepared for flow cytometry. Peptide-pulsed and -unpulsed target cells were identified by their differential CFSE intensity. Up to 10^4 CFSE-positive cells were collected for analysis. Specific lysis was quantified with the following formula: % specific lysis = $[1-(R_{naive}/R_{immunized})] \times 100$, where R = % $CFSE^{low}$ cells/% $CFSE^{high}$ cells.

CFSE-labeling and T cell proliferation assays. FACS-sorted naïve OT-I or OT-II cells were incubated with CFSE (5 μM; Molecular Probes) for 10 min at 37°C and thoroughly washed. CFSE-labeled cells were injected into recipient mice (5×10^5 per mouse) or co-cultured (10^5 per sample) with other cells in vitro and were harvested 64 hours after in vivo vaccination or in vitro co-culture. Cell proliferation based on CFSE dilution was analyzed using FlowJo software. Responder frequency (R) and proliferative capacity (Cp) were calculated as previously described (2).

Cell isolation from multiple organs for phenotyping. Mice were perfused systemically with PBS via the left and right ventricles. Lungs, livers and spleens were dissolved with HBSS medium containing 5% FBS, 10 mM HEPES, collagenase A (1 mg/ml; Roche) and DNase I (0.4-0.6 mg/ml; Roche) for 30 minutes at 37°C by gentle shaking, minced, passed through a 70 μm cell strainer, and RBC lysed with ACK buffer. Lymph node (LN) samples were pooled from bilateral inguinal and popliteal LN (n=4) and prepared as described above except no RBC lysis was required. Single-cell suspensions of BM samples were prepared from femoral bones with an RBC lysis process and cell strainer filtering. Mononuclear blood cell-enriched samples were prepared by density gradient centrifugation methods with Lymphocyte Separation Medium (LSM, density = 1.077-1.08 g/ml at 20°C; Cellgro).

Co-culture of autologous human monocytes, lymphocytes and DC. Highly-enriched human monocytes (>80%) and lymphocytes (>95%) were obtained from two CMV-positive donors by elutriation with a cell separator (Elutra^{TM}; Terumo BCT, Lakewood, CO) (3). After collection, the cells were frozen and assessed for contamination and lineage purity as previously described (4). Autologous DC were generated from monocytes in AIM V medium (Gibco) containing GM-CSF (800 U/ml) and IL-4 (500 U/ml) as previously described (5). The 1.932-kb CMV pp65 full-length cDNA insert was obtained from B. Britt and RNA was generated as previously described (5). To transfect monocytes, mRNA was used at a dose of 5 μg per 10^6 cells. CMV pp65-mRNA was thoroughly mixed with Lipofectamine MessengerMax (Invitrogen) at a ratio of 1:4 (w/v) after both were diluted 10-fold in Opti-MEM medium (Gibco). The lipid-mRNA mixture was incubated at room temperature for 5 minutes and then added into monocyte suspensions (10^6/ml) in AIM V medium with 10% FBS (the culture medium) for a 2-hour incubation with 5% CO_2 at 37°C. Post incubation, monocytes were washed thoroughly with PBS and resuspended in culture medium. Autologous CMV pp65 RNA-transfected human monocytes, CFSE-labeled lymphocytes (10^5) and/or DC (all at a number of 10^5 cells per well) were co-cultured in a 96-well plate with 5% CO_2 at 37°C for 64 hours before flow cytometric analysis of T cell proliferation.

Time-lapse live imaging of monocyte-cDC co-culture. DQ-OVA-loaded mouse monocytes and FACS-sorted mouse splenic cDC were co-cultured in a 1:1 ratio in cRPMI-20 medium for 18 hours. A fixed field of the culture dish was continuously imaged with a Zeiss Axio Observer Z1. The images were processed and analyzed on MetaMorph and FIJI.

Immunofluorescence. Freshly harvested spleens were frozen in OCT. Frozen sections of 10 μm-thickness were stained with the following primary antibodies: rat anti-mouse CD169 (3D6.112; BioLegend), rat anti-mouse CD8α (53-6.7; Invitrogen), rabbit anti-mouse CD3 (SP7; Abcam), Armenian hamster anti-mouse CD11c (N418; eBioscience), biotinylated mouse anti-mouse CD45.2 (104; eBioscience) and rabbit anti-mouse connexin 43 (polyconal, affinity purified; Sigma). The secondary antibodies were Dylight 488-conjugated goat anti-Armenian hamster IgG, AF488-conjugated goat anti-rat IgG (both from BioLegend), AF488-conjugated donkey anti-rabbit IgG, AF546-conjugated goat anti-rat IgG, AF555- conjugated donkey anti-rabbit IgG, AF568-conjugated goat anti-hamster IgG and AF647-conjugated streptavidin (all from Invitrogen). Control staining of connexin 43 was performed with normal rabbit IgG (Santa Cruz) as primary antibody plus AF488-conjugated donkey anti-rabbit IgG. To quantify OVA-loaded monocyte-splenic cDC interactions or localization of OVA-loaded monocytes in the spleen, 5 low-power fields continuous from one end to the other end of a sagittal-cut spleen section were imaged with 3 spleen sections per mouse (total 15 fields per mouse and 3 mice per group). The percentage of $CD8^+$ cDC-contacting monocytes among total injected OVA-

monocytes in each low-power field was recorded. Confocal images were obtained using a Leica SP5 inverted confocal microscope and analyzed on Imaris and Fiji/ImageJ.

Tetanus-diphtheria (Td) toxoid Immunizations and DC vaccination. DC vaccination was performed as previously described (6). Female 6-8 week-old C57BL/6 mice received a primary IM injection of Td toxoid (Sanofi Aventis; Tenivac®; 1 Lf, 100 µl) bilaterally into the quadriceps muscle (50 µl per leg). An IM booster (0.5 Lf, 50 µl) was administered two weeks later. Vaccine site pre-conditioning with Td toxoid (0.5 Lf) was given SQ two weeks after the booster and randomized to the right or left groin site. DC were resuspended at 10^6/100 µl PBS and administered SQ on both sides 0.8 cm from the groin crease 24 hours after pre-conditioning.

Quantitative real-time PCR. Total RNA was extracted from FACS-sorted splenic cDC, monocytes and monocyte-derived DC by using RNeasy® Plus Mini Kit (Qiagen). RNA was reverse transcribed with QuantiTect® Reverse Transcription Kit (Qiagen). Quantitative PCR was performed with PowerUp™ SYBR™ Green Master Mix reagent (Applied Biosystems) on an Applied Biosystems 7300 Real-Time PCR System (Applied Biosystems). The expression of connexin isoform genes was normalized to ribosomal protein L32 (*Rpl32*) (7) and the PCR performed in triplicate. Results were quantified by the $2^{-\Delta\Delta CT}$ method (8). The primer sequences of 20 different murine connexin isoform genes and *Rpl32* are the same as previously published (7).

Supplemental Reference

1. Lin KL, Sweeney S, Kang BD, Ramsburg E, and Gunn MD. CCR2-antagonist prophylaxis reduces pulmonary immune pathology and markedly improves survival during influenza infection. *J Immunol.* 2011;186(1):508-15.
2. Gudmundsdottir H, Wells AD, and Turka LA. Dynamics and requirements of T cell clonal expansion in vivo at the single-cell level: effector function is linked to proliferative capacity. *J Immunol.* 1999;162(9):5212-23.
3. Berger TG, Strasser E, Smith R, Carste C, Schuler-Thurner B, Kaempgen E, et al. Efficient elutriation of monocytes within a closed system (Elutra) for clinical-scale generation of dendritic cells. *J Immunol Methods.* 2005;298(1-2):61-72.
4. Thurner B, Roder C, Dieckmann D, Heuer M, Kruse M, Glaser A, et al. Generation of large numbers of fully mature and stable dendritic cells from leukapheresis products for clinical application. *J Immunol Methods.* 1999;223(1):1-15.
5. Nair S, Archer GE, and Tedder TF. Isolation and generation of human dendritic cells. *Current protocols in immunology / edited by John E Coligan [et al].* 2012;Chapter 7:Unit7 32.
6. Mitchell DA, Batich KA, Gunn MD, Huang MN, Sanchez-Perez L, Nair SK, et al. Tetanus toxoid and CCL3 improve dendritic cell vaccines in mice and glioblastoma patients. *Nature.* 2015;519(7543):366-9.
7. Mazzini E, Massimiliano L, Penna G, and Rescigno M. Oral tolerance can be established via gap junction transfer of fed antigens from CX3CR1(+) macrophages to CD103(+) dendritic cells. *Immunity.* 2014;40(2):248-61.
8. Pfaffl MW. A new mathematical model for relative quantification in real-time RT-PCR. *Nucleic Acids Res.* 2001;29(9):e45.

Supplemental Figures

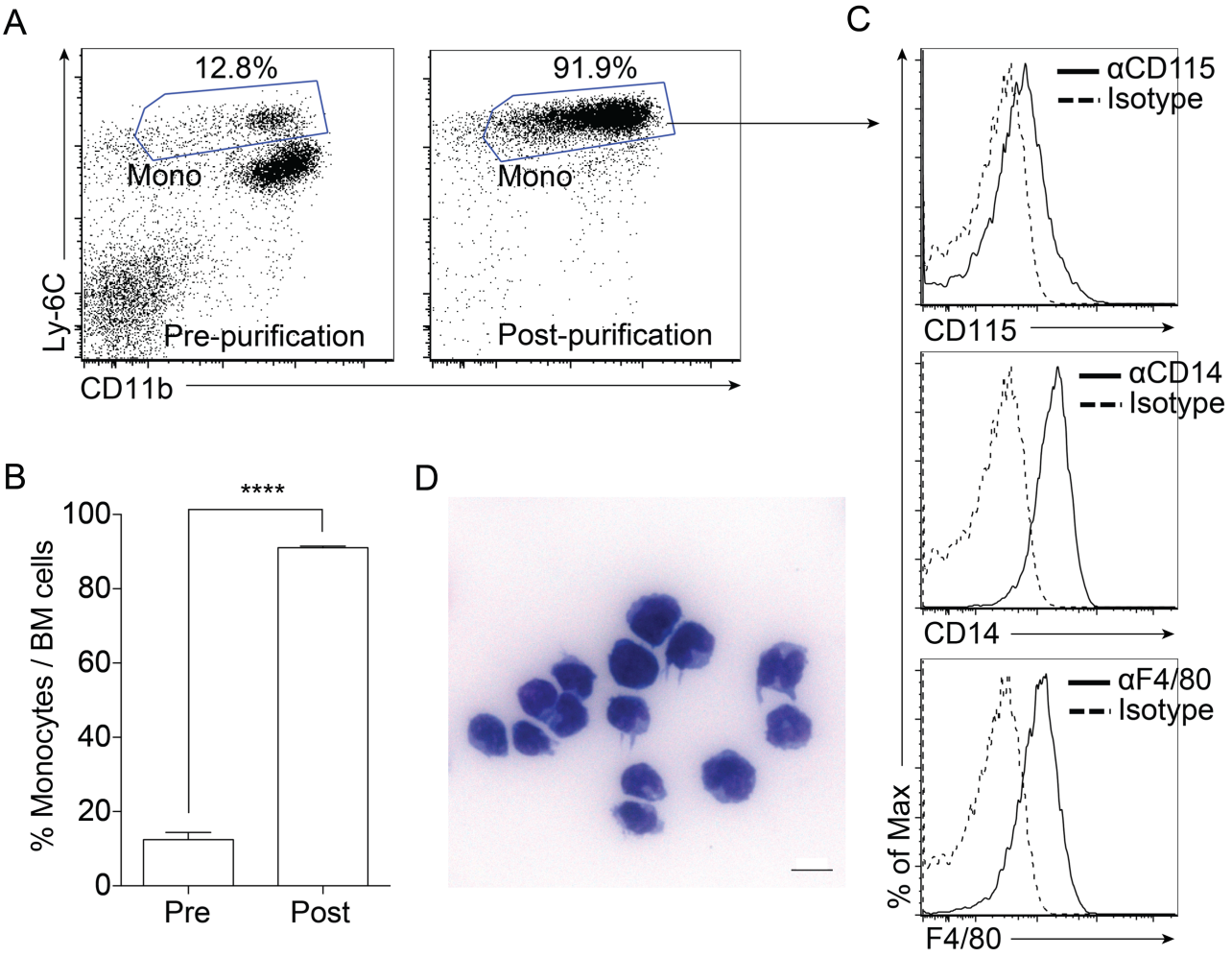

Supplemental Figure 1. Purification of murine classical Ly-6C^{hi} monocytes from BM.

Murine classical Ly-6C^{hi} monocytes were purified from BM cells via negative selection with MACS columns. (A) Representative dot plots showing percentages of classical Ly-6C^{hi} monocytes among total BM cells pre- and post-purification. (B) The graph derived from (A) showing monocyte purity pre- and post-purification. N=3 per group. **** $P < 0.0001$ (unpaired two-tailed Student's *t*-test). Data represent mean ± sem. (C) The phenotype of purified monocytes. (D) The morphology of purified monocytes (Wright-Giemsa equivalent staining; scale bar: 10 μm).

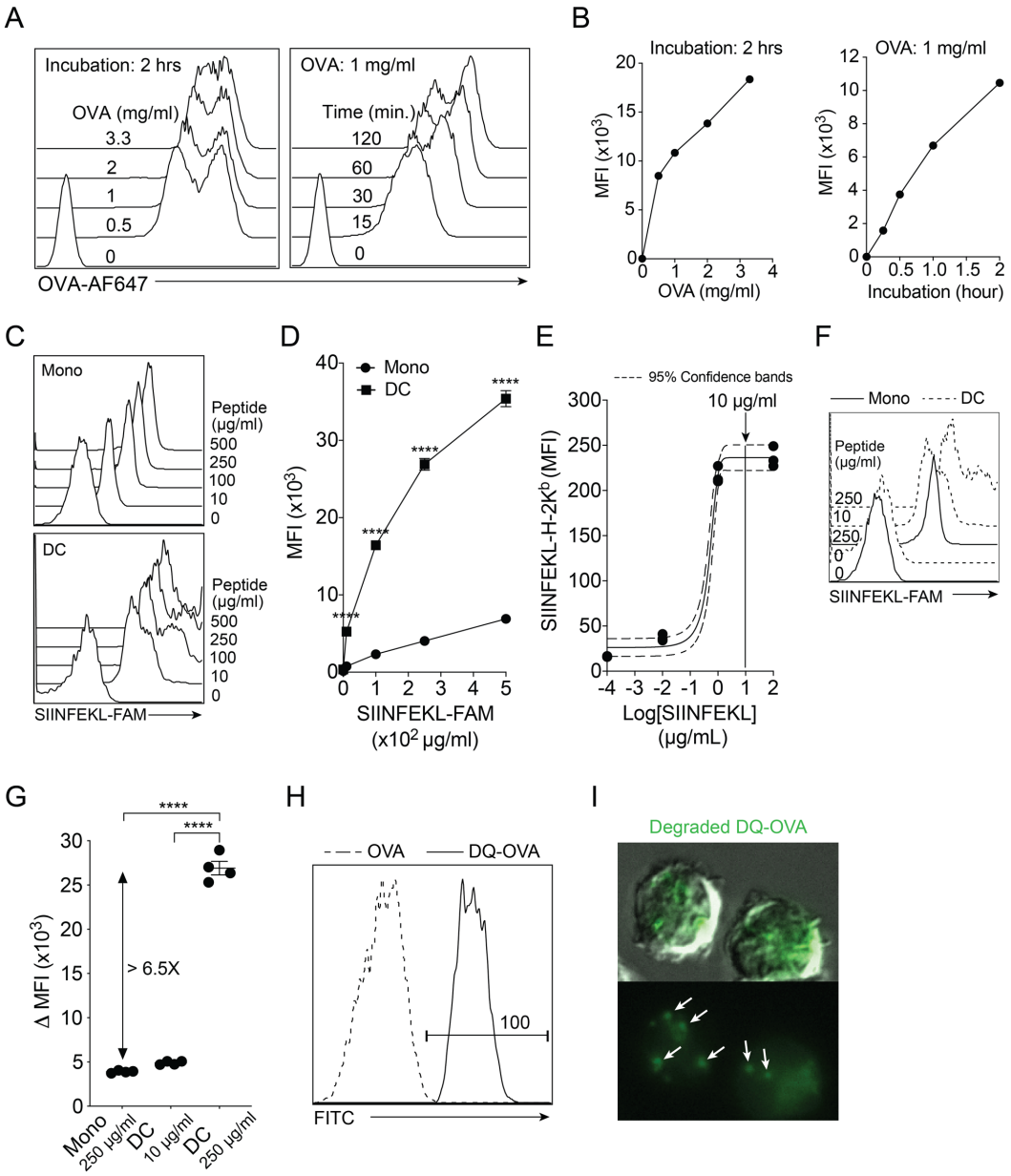

Supplemental Figure 2. Antigen loading on monocytes.
Monocytes (A-D, F-I) or BM-derived DC (C-G) were incubated ex vivo with fluorophore-conjugated Ag for Ag uptake analysis. (A) Representative flow cytometric histograms showing AF647-conjugated OVA uptake of monocytes at increasing Ag concentrations and incubation time. (B) Graphs derived from (A) (MFI: geometric mean fluorescent intensity). (C) Representative histograms showing SIINFEKL-FAM uptake of monocytes and DC at increasing Ag concentrations after 2-hour incubation. (D) The graph derived from (C). N=4 per group. Data represent mean ± sem. Monocyte vs. DC at each concentration. **** $P < 0.0001$ (two-way ANOVA with Bonferroni's test). (E) Graph derived from a flow cytometric analysis of Ag presentation by MHCI on DC by cell surface staining with a monoclonal antibody specifically against SIINFEKL-H-2K^b complex at increasing Ag concentrations after 2-hour incubation in vitro. N=3 per group. Data are analyzed with non-linear regression and presented as a best-fit curve with 95% confidence bands. (F) Representative histogram derived from (C). (G) The graph derived from (F). **** $P < 0.0001$ (one-way ANOVA with Tukey's test). Data represent mean ± sem. (H) Representative histogram showing DQ-OVA degradation occurs in 100% of monocytes after 1.5-hour incubation. (I) A snapshot from a time-lapse live imaging on monocytes incubated with DQ-OVA showing vesicular containment and phagoendosomal degradation of OVA (arrows).

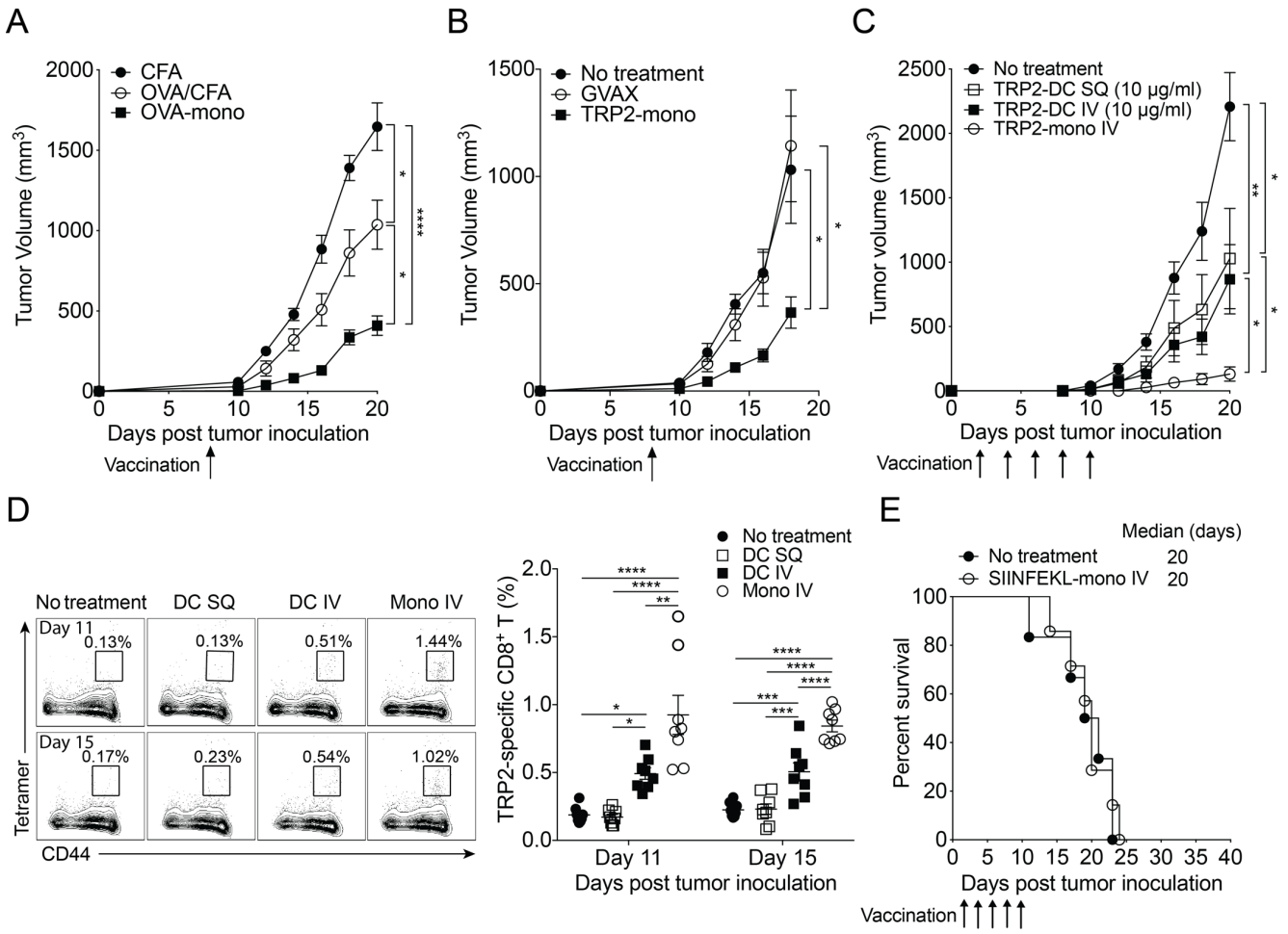

Supplemental Figure 3. Comparison of anti-tumor efficacy between Ag-loaded monocytes and conventional cancer vaccines.

(A,B) Mice were SQ inoculated with B16/F10-OVA ($2x10^5$) (A) and B16/F10 ($5x10^4$) (B) melanoma cells 8 days before received single shot of various therapeutic vaccines. (A) Tumor growth curves of mice treated with SQ CFA, SQ OVA (200 μg) in CFA (OVA/CFA) or IV $3x10^6$ of OVA-loaded monocytes (OVA-mono). N=15 per group. (B) Tumor growth curves of mice untreated (no treatment), treated with SQ $3x10^6$ irradiated GM-CSF-secreting B16/F10 cells (GVAX) or IV $3x10^6$ $TRP2_{180-188}$-loaded monocytes (TRP2-mono). N=10 per group. (C) Growth of SQ B16/F10 melanoma tumors ($5x10^4$) in mice untreated (no treatment) or vaccinated every other day beginning 2 days post tumor inoculation for total 5 doses of SQ 10^6 $TRP2_{180-188}$-loaded (10 μg/ml) DC (TRP2-DC SQ), IV 10^6 $TRP2_{180-188}$-loaded (10 μg/ml) DC (TRP2-DC IV) or IV 10^6 $TRP2_{180-188}$-loaded monocytes (TRP2-mono IV). N=8 per group. (D) Frequency of TRP2-specific ($TRP2_{180-188}$-H-$2K^b$ tetramer$^+$) $CD8^+$ T cells among total blood $CD8^+$ T cells at the indicated time points of the experiment in (C). * $P < 0.05$, ** $P < 0.01$, *** $P < 0.001$, **** $P < 0.0001$ (one-way ANOVA with Tukey's test). (A-C) Tumor size comparisons: * $P < 0.05$, ** $P < 0.01$, **** $P < 0.0001$ (unpaired two-tailed Student's *t*-test). Data represent mean ± sem. (E) Survival of the mice IC inoculated with TRP2-expressing CT-2A astrocytoma cells ($5x10^4$) either untreated (no treatment) or treated with 5 doses of SIINFEKL-loaded monocyte (SIINFEKL-mono IV) vaccination every other day beginning on day 2 post tumor inoculation. N=8 per group. Median: median survival days. No statistical significance of survival curves by Log-rank test.

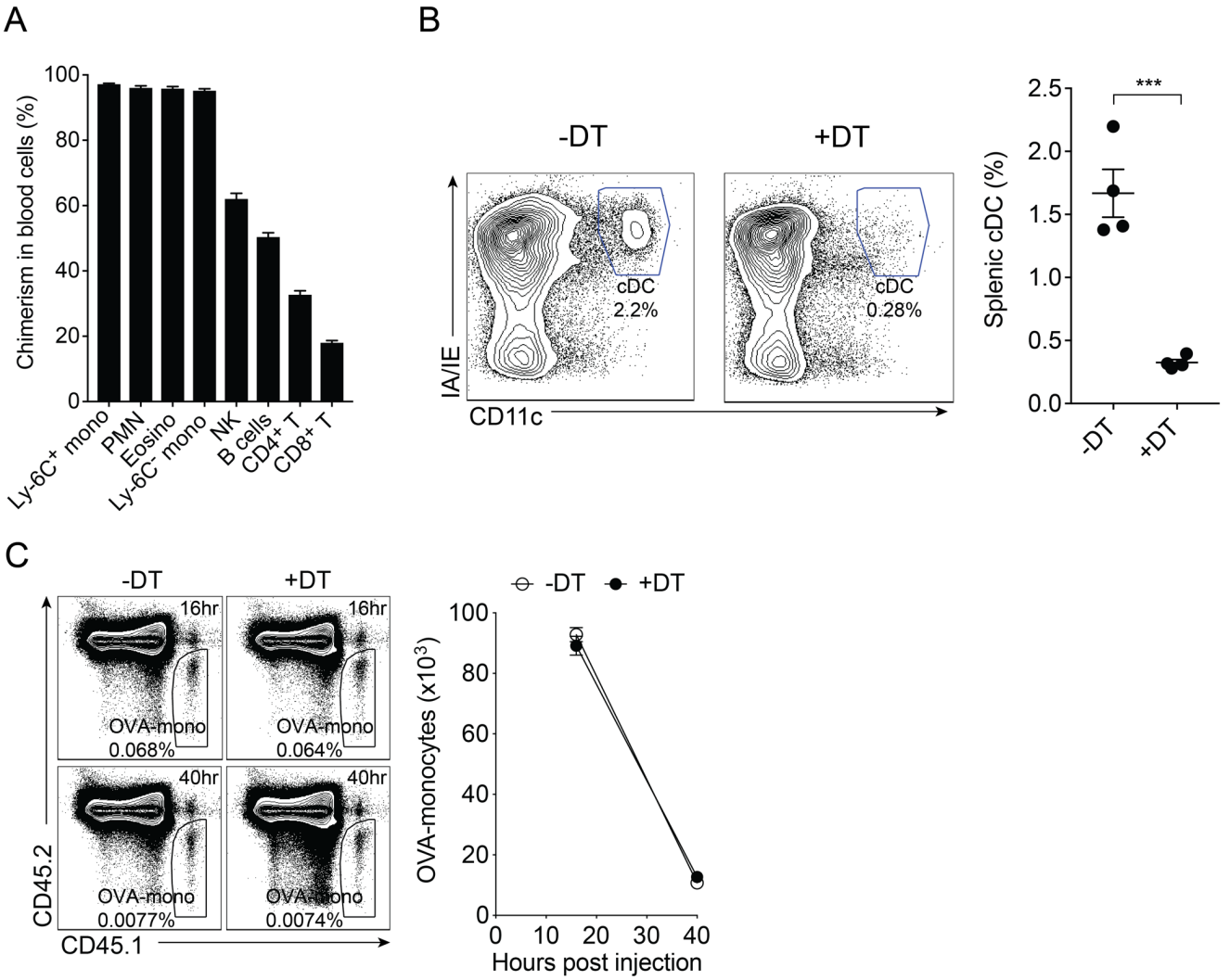

Supplemental Figure 4. The phenotype of zDC-DTR BM chimeric mice.

To generate zDC-DTR BM chimeric mice, T cell-depleted BM cells from zDC-DTR homozygous mice (CD45.2) were IV injected into CD45.1 congenic (A,B) or CD45.2 isogenic (C) mice which had been myeloablated with busulfan. (A) Chimerism was checked 4 weeks after zDC-DTR BM cell injection with flow cytometry based on the percentages of CD45.2 cells among various blood cells. Eosino: eosinophils; mono: monocytes; PMN: polymorphonuclear neutrophils. (B) Representative flow cytometric contour plots and their derived graph showing percentages of splenic cDC among total live splenocytes on day 2 post IP injection of PBS (-DT) or DT (+DT) (25 ng/g) in zDC-DTR BM chimeras. *** $P < 0.001$ (unpaired two-tailed Student's *t*-test). (C) OVA-loaded CD45.1 monocytes ($2x10^6$; OVA-mono) were IV injected on day 2 post IP injection of PBS (-DT) or DT (+DT) (25 ng/g) in zDC-DTR BM chimeras. Representative flow cytometric contour plots and their derived graph respectively showing percentages among total live splenocytes and cell numbers of OVA-mono in the spleen at 16 and 40 hours post injection. No statistical significance by two-way ANOVA with Bonferroni's test. Data represent mean ± sem.

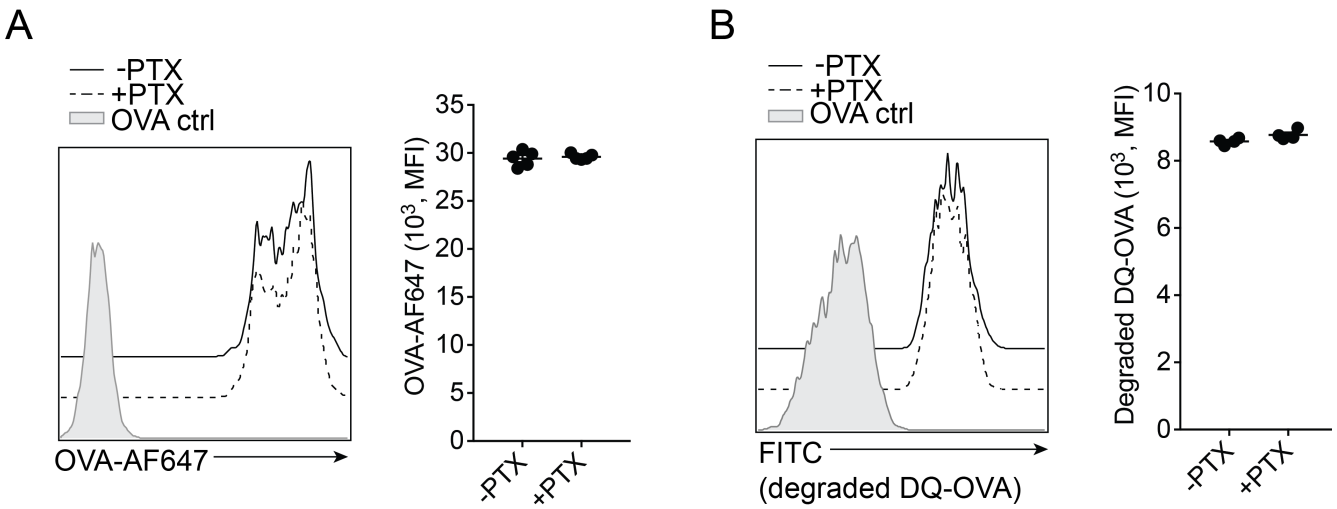

Supplemental Figure 5. PTX treatment does not affect ex vivo Ag uptake and processing of monocytes.

Monocytes were incubated ex vivo for 1.5 hours with unconjugated OVA protein (OVA ctrl), AF647-conjugated OVA (OVA-AF647) (A) or DQ-OVA (B). (A) Representative flow cytometric histogram and the derived graph showing OVA uptake of monocytes with (+) or without (-) PTX in the incubation. (B) The FITC fluorescent intensity of auto-quenched DQ-OVA is parallel to the magnitude of its degradation (i.e. Ag processing) in the monocytes. Representative histogram and the derived graph showing the intensity of OVA degradation in the monocytes with (+) or without (-) PTX in the incubation. No statistical significance was found (unpaired two-tailed Student's *t*-test). Data represent mean ± sem.

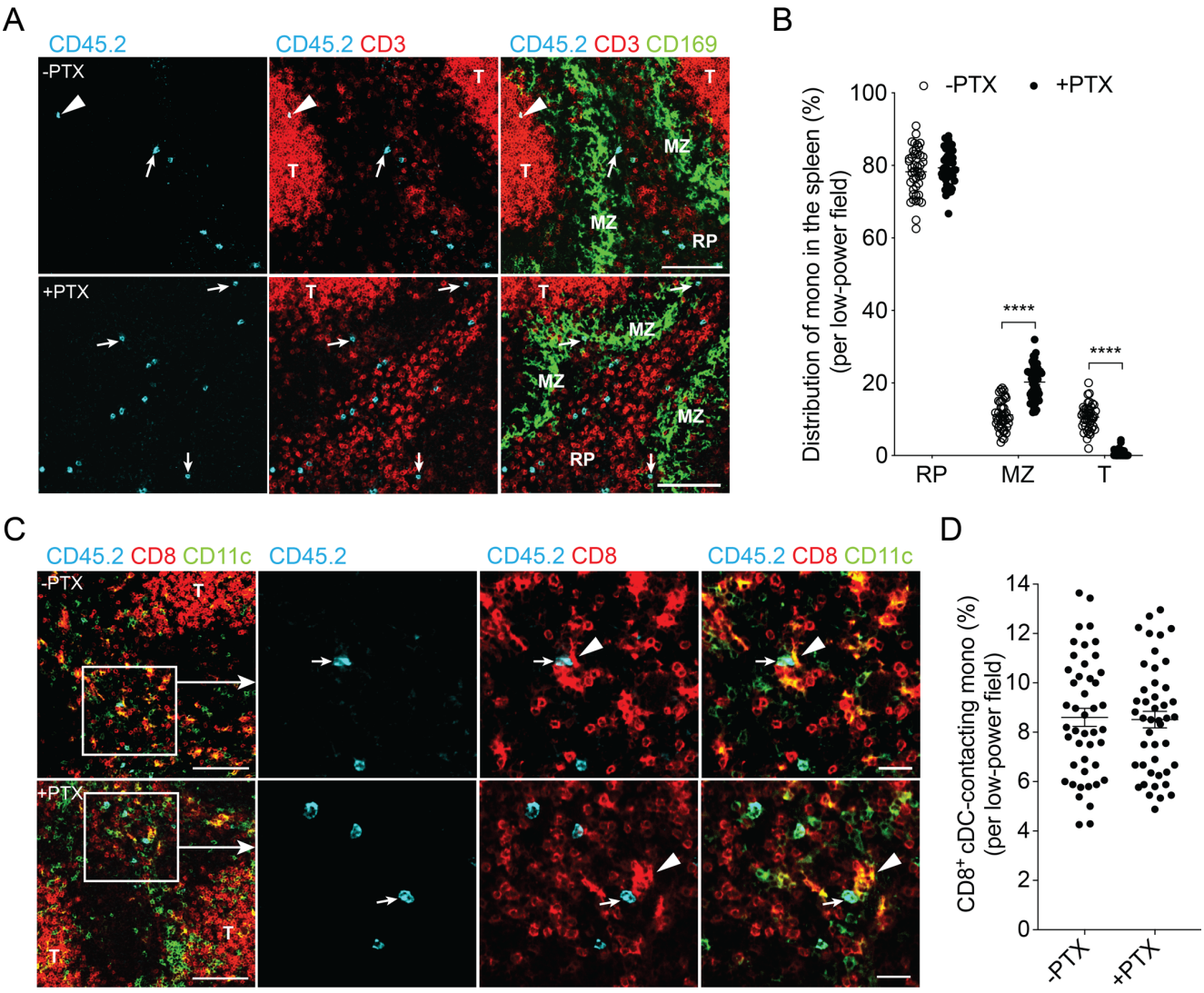

Supplemental Figure 6. PTX treatment on monocytes does not disrupt monocyte-CD8$^+$ cDC engagement in the spleen.

(A-D) PTX-untreated (-) or -treated (+) CD45.2 OVA-monocytes (2x10^6) were IV injected into CD45.1 mice and the spleens were harvested at 16 hours post monocyte injection. (A) Representative immunofluorescent micrographs of spleen sections showing OVA-monocytes in the T cell zones (arrowheads), MZ (arrows) and RP (unlabeled cyan cells). MZ: marginal zone; RP: red pulp; T: T cell zone. Scale bar: 100 μm. (B) The distribution of OVA-monocytes in RP, MZ and T cell zones based on numeration of OVA-monocytes of the spleen sections in low-power fields. Total 45 low-power fields (15 fields per mouse) were taken from 3 mice per group. **** $P < 0.0001$ (two-way ANOVA with Bonferroni's test). (C) Representative immunofluorescent micrographs of spleen sections showing OVA-monocytes (arrows) making physical contacts with CD8$^+$ cDC (arrowheads). Scale bars: 100 μm (original images), 25 μm (insets). (D) The percentages of CD8$^+$ cDC-contacting OVA-monocytes among total OVA-monocytes in low-power fields. Total 45 low-power fields (15 fields per mouse) were taken from 3 mice per group. T: T cell zone. No statistical significance between two groups (unpaired two-tailed Student's *t*-test). Data represent mean ± sem.

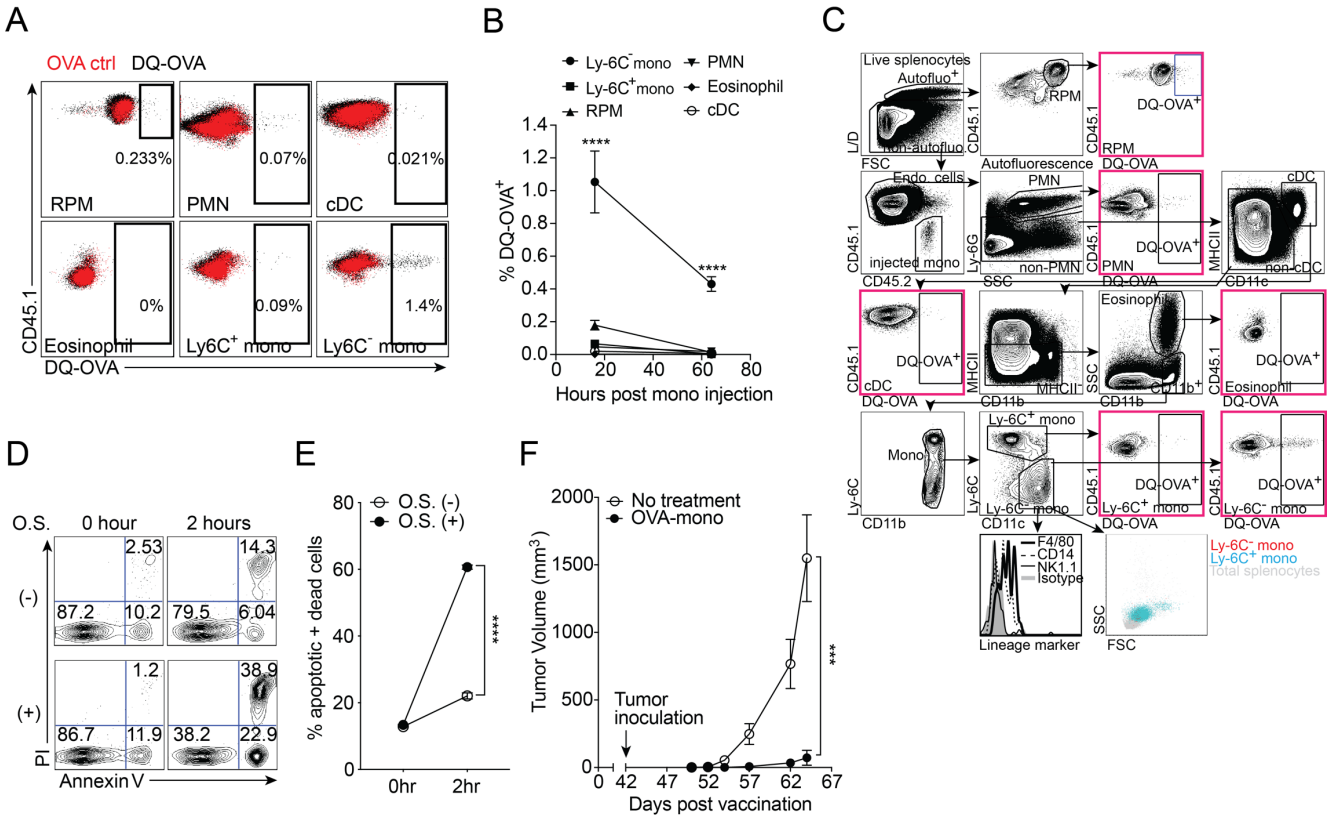

Supplemental Figure 7. Monocytes do not transfer Ag in bulk to splenic cDC via phagocytosis.

(A,B) Monocytes loaded with DQ-OVA or unconjugated OVA (OVA ctrl) were IV injected into CD45.1 congenic mice 16 hours (A,B) or 64 hours (B) prior to spleen harvest for flow cytometry. cDC: conventional DC; mono: monocytes; RPM: red pulp macrophages; PMN: polymorphonuclear neutrophil. (A) Representative dot plots showing uptake of monocyte-derived processed OVA (fluorescently positive DQ-OVA) in various endogenous splenocytes. Numbers in the plots are the percentages of DQ-OVA positive cells among the indicated cell types. (B) Frequency of DQ-OVA uptake among different endogenous splenocytes over time. **** $P < 0.0001$ (Ly-6C$^-$ mono vs. all the other cell types; one-way ANOVA with Tukey's test). (C) The gating strategy used in (A). Live splenocytes are gated for further downstream phenotyping. The validity of Ly-6C$^-$ monocyte gate is corroborated by the analysis of several lineage-specific marks and their cell size and granularity. cDC: conventional DC; FSC: forward-scattered light; SSC: side-scattered light; L/D: Live/Dead dye. Mono: monocyte. PMN: polymorphonuclear neutrophil. RPM: red pulp macrophage. (D) OVA-loaded monocytes treated without (-) or with (+) osmotic shock (O.S.) were cultured in vitro for 2 hours. Representative contour plots showing apoptosis (Annexin$^+$PI$^-$) and cell death (Annexin$^+$PI$^+$) of OVA-loaded monocytes in the indicated conditions at 0 and 2 hours in culture. Numbers are the percentages of total OVA-monocytes. PI: propidium iodide. (E) The frequency plot derived from (D). N=3 per group. **** $P < 0.0001$ (two-way ANOVA with Bonferroni's test). (F) Growth of SQ B16/F10-OVA melanoma tumors in mice untreated (no treatment) or treated with OVA-monocyte vaccination (IV 3x10^6; OVA-mono) 42 days prior to tumor inoculation. N=9 per group. Tumor size comparison: *** $P < 0.001$ (unpaired two-tailed Student's *t*-test). Data represent mean ± sem.

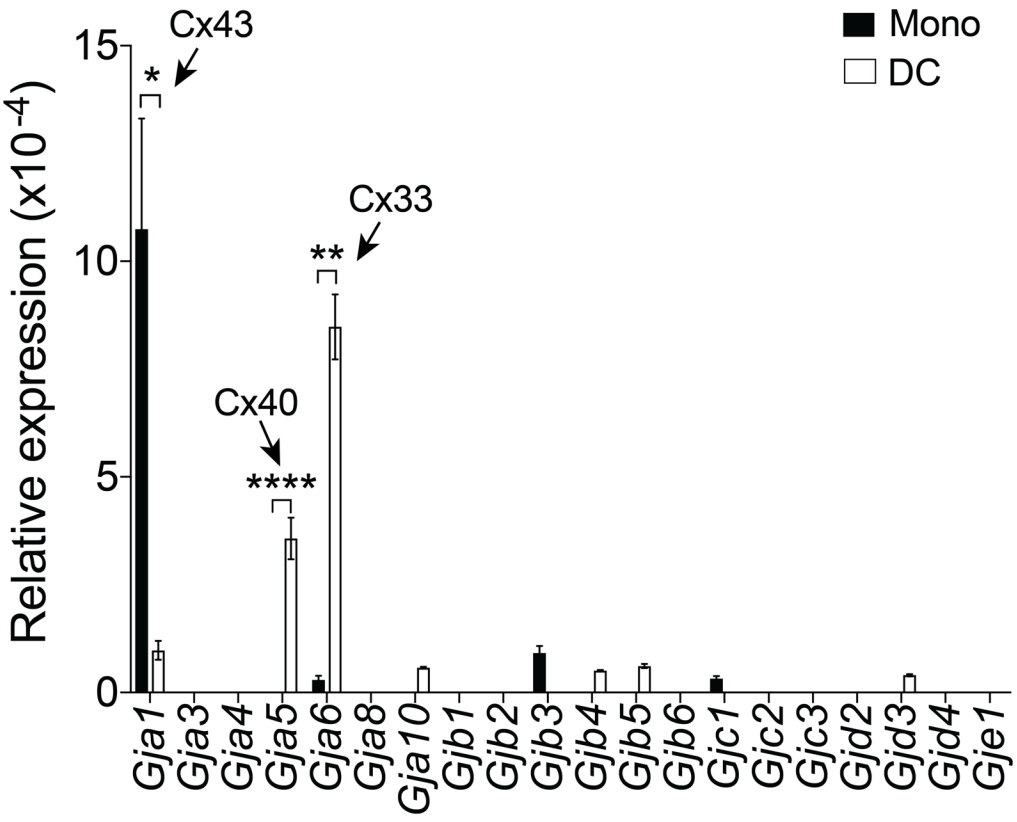

Supplemental Figure 8. Expression of connexin isoforms in monocytes and monocyte-derived DC.

Relative mRNA expression of connexin (Cx) isoforms was evaluated in mouse monocytes (mono) and monocyte-derived DC (DC) by qPCR and normalized to *Rpl32* housekeeping gene using the $2^{-\Delta\Delta CT}$ method. Monocyte-derived DC was generated ex vivo with GM-CSF + IL-4. N=3 per group. * $P < 0.05$, ** $P < 0.01$, **** $P < 0.0001$ (unpaired two-tailed Student's *t*-test). Data represent mean ± s.e.m.

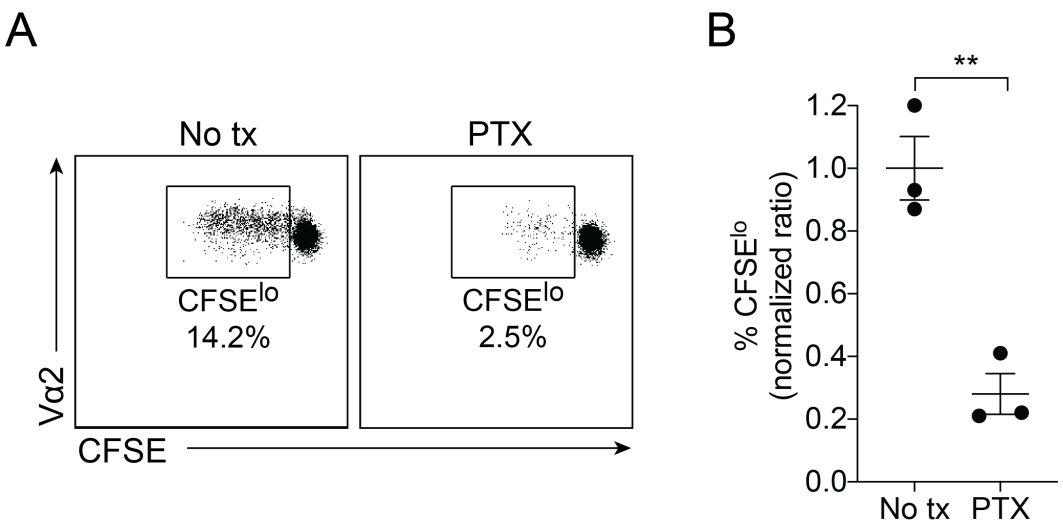

Supplemental Figure 9. PTX effect on OT-I cell priming in the in vitro co-culture with monocytes and splenic cDC.

CFSE-labeled naïve OT-I cells (10^5) were in vitro co-cultured with OVA-loaded MHCI-deficient monocytes (10^5) and splenic cDC (10^5) for 64 hours as described in Figure 7D before flow cytometric analysis. (A) Representative dot plots showing percentages of proliferating OT-I cells ($CFSE^{lo}$) among total OT-I cells in the absence (no tx) or presence of PTX (100 ng/ml). (B) The scatter plot derived from (A). The percentages of proliferating CFSE-labeled OT-I cells ($CFSE^{lo}$) are normalized to the mean percentage of the no treatment group (no tx). ** $P < 0.01$ (unpaired two-tailed Student's *t*-test). Data represent mean ± s.e.m.

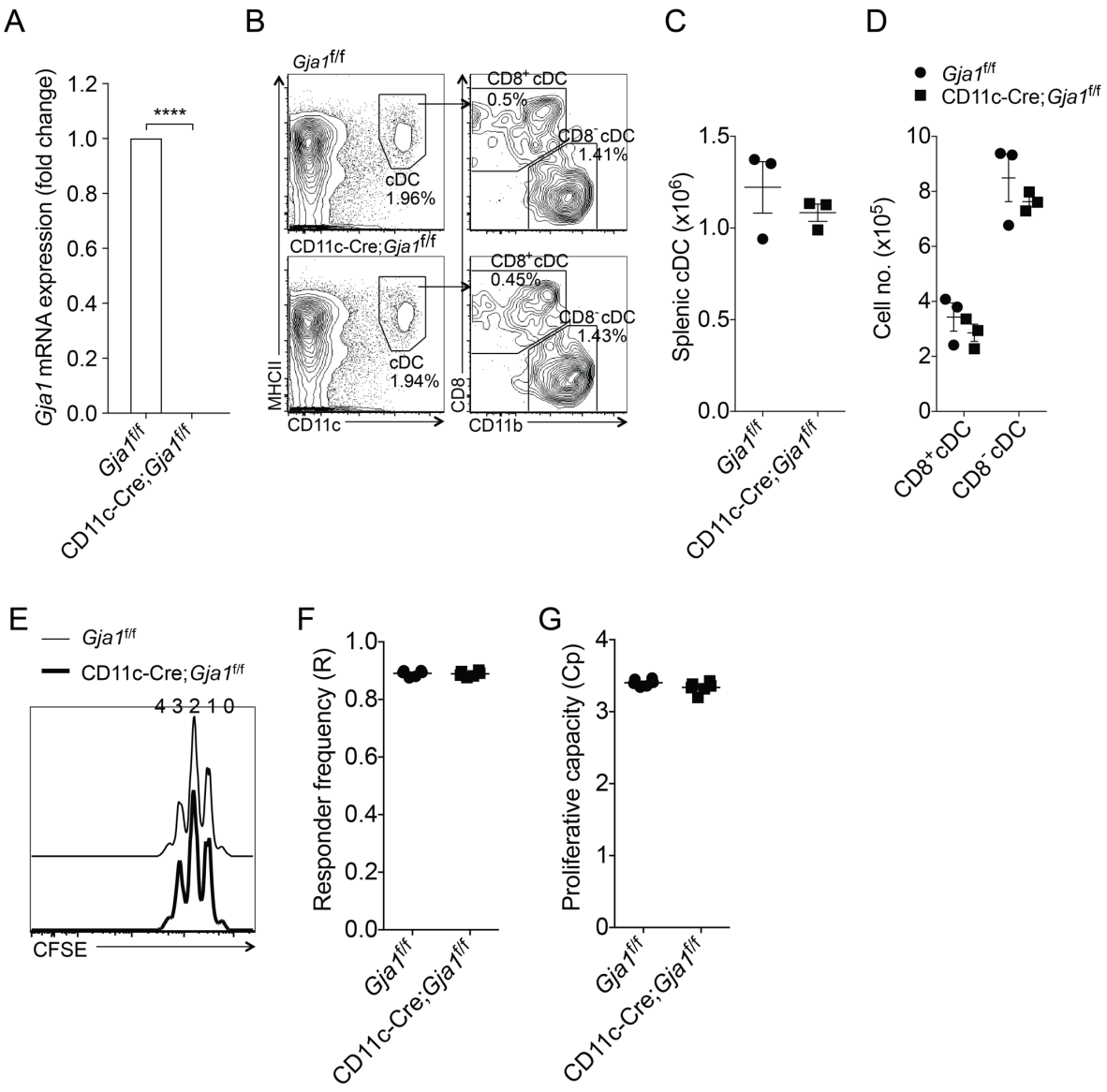

Supplemental Figure 10. The phenotype of CD11c-Cre;*Gja1*$^{f/f}$ mice.

(A) Relative Cx43 (*Gja1*) mRNA expression of splenic cDC revealed by real-time PCR. N=3 per group. **** $P < 0.0001$ (unpaired two-tailed Student's *t*-test). (B) Representative contour plots showing frequencies of total cDC, $CD8^+$ and $CD8^-$ cDC subsets among total live splenocytes. (C,D) Cell numbers of total splenic cDC (C) and cDC subsets (D) converted from the frequencies shown in (B). (E) Representative histograms showing proliferation of CFSE-labeled OT-I cells being stimulated in vitro by SIINFEKL-pulsed splenic cDC for 64 hours. The numbers on top of the histogram indicate the proliferating generations of OT-I cells. (F,G) Graphs derived from (E) showing responder frequency of OT-I cells (F) and proliferative capacity of those responding OT-I cells (G) being stimulated by the SIINFEKL-pulsed splenic cDC of the indicated genotypes. No statistical significance was found by two-way ANOVA with Bonferroni's test (the panel of D) and unpaired two-tailed Student's *t*-test (the panels of C, F, G). Data represent mean ± s.e.m.

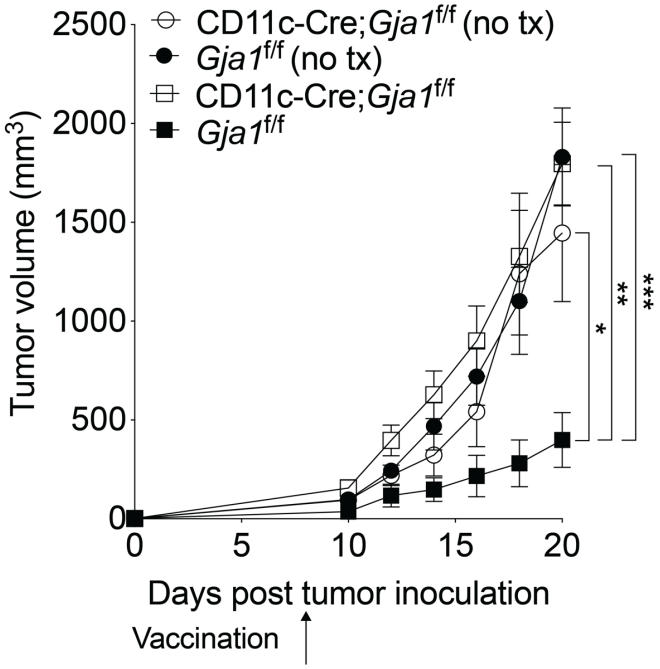

Supplemental Figure 11. Anti-tumor efficacy of monocyte vaccination in mice with gap junction-intact or -deficient cDC.

Growth of SQ B16/F10-OVA melanoma tumors ($2x10^5$) in mice of the indicated genotypes untreated (no tx) or vaccinated with IV OVA-monocytes ($3x10^6$ per mouse x 1) on day 8 post tumor inoculation. N=5 per group. Tumor size comparison: * $P < 0.05$, ** $P < 0.01$, *** $P < 0.001$ (unpaired two-tailed Student's *t*-test). Data represent mean ± sem. *Gja1*: the gene of Cx43.

Supplemental Movie Legend

Supplemental Movie 1. Splenic cDC actively approaching Ag-loaded monocytes with long-lasting physical contacts.

The full video clip for Figure 5B. Monocytes were loaded/labeled with DQ-OVA (arrows) and co-cultured with FACS-sorted unlabeled splenic cDC (arrowheads). Auto-quenched DQ-OVA was degraded in the vesicular structures of the monocytes, releasing dot-like green fluorescence. Time display at right lower corner of the frame is shown as hh:mm.